UNCLASSIFIED
SECURITY CLASSIFICATION OF THIS PAGE

MASTER COPY — FILE COPY — FOR REPRODUCTION PURPOSES

(2)

AD-A217 798 REPORT DOCUMENTATION PAGE

1a. REPORT SECURITY CLASSIFICATION: Unclassified	1b. RESTRICTIVE MARKINGS
2a. SECURITY CLASSIFICATION AUTHORITY	3. DISTRIBUTION / AVAILABILITY OF REPORT: Approved for public release; distribution unlimited.
2b. DECLASSIFICATION / DOWNGRADING SCHEDULE	
4. PERFORMING ORGANIZATION REPORT NUMBER(S)	5. MONITORING ORGANIZATION REPORT NUMBER(S): ARO 23617.3-MS
6a. NAME OF PERFORMING ORGANIZATION: University of Wisconsin-Madison; 6b. OFFICE SYMBOL (If applicable)	7a. NAME OF MONITORING ORGANIZATION: U. S. Army Research Office
6c. ADDRESS (City, State, and ZIP Code): Dept. of Materials Science and Engineering, 1509 University Avenue, Madison, WI 53706	7b. ADDRESS (City, State, and ZIP Code): P. O. Box 12211, Research Triangle Park, NC 27709-2211
8a. NAME OF FUNDING / SPONSORING ORGANIZATION: U. S. Army Research Office; 8b. OFFICE SYMBOL (If applicable)	9. PROCUREMENT INSTRUMENT IDENTIFICATION NUMBER: DAAL03-86-K-0114
8c. ADDRESS (City, State, and ZIP Code): P. O. Box 12211, Research Triangle Park, NC 27709-2211	10. SOURCE OF FUNDING NUMBERS: PROGRAM ELEMENT NO. / PROJECT NO. / TASK NO. / WORK UNIT ACCESSION NO.

11. TITLE (Include Security Classification): Undercooling of Aluminum Alloys

12. PERSONAL AUTHOR(S): Perepezko, J. H., Furrer, D. U.

13a. TYPE OF REPORT	13b. TIME COVERED	14. DATE OF REPORT (Year, Month, Day)	15. PAGE COUNT
~~Reprint~~	FROM 86/7/1 TO 89/6/30	1988, October	26

16. SUPPLEMENTARY NOTATION: The view, opinions and/or findings contained in this report are those of the author(s) and should not be construed as an official Department of the Army position, policy, or decision, unless so designated by other documentation.

17. COSATI CODES			18. SUBJECT TERMS (Continue on reverse if necessary and identify by block number)
FIELD	GROUP	SUB-GROUP	Aluminum Alloys, Powders, Microstructure, Solidification Kinetics, Undercooling, Dispersion Strengthening, Thermal History, Nucleation, Eutectic Structures

19. ABSTRACT (Continue on reverse if necessary and identify by block number)

The development of refined microstructures for dispersion strengthening of Al alloys by rapid solidification is related to the undercooling at nucleation and during competitive crystal growth. With controlled droplet samples the important processing parameters that govern undercooling in the powders have been identified and include powder size and coating, melt cooling rate and superheat. The droplet method has yielded measured undercoolings of 175°C for Al and values near 300°C for some Al alloys. Droplet studies have been valuable in examining the solidification pathways including thermal history effects associated with rapid solidification and dispersoid formation in Al-Ni, Al-Fe, and Al-Be alloys. Based on the analysis of solidification pathways, microstructure maps may be developed to identify the processing that can yield fine-scale eutectics, metastable structures or suppression of coarse primary intermetallic phases which are useful for the development of dispersoid structures.

20. DISTRIBUTION / AVAILABILITY OF ABSTRACT: ☐ UNCLASSIFIED/UNLIMITED ☐ SAME AS RPT. ☐ DTIC USERS	21. ABSTRACT SECURITY CLASSIFICATION: Unclassified
22a. NAME OF RESPONSIBLE INDIVIDUAL	22b. TELEPHONE (Include Area Code) / 22c. OFFICE SYMBOL

DD FORM 1473, 84 MAR — 83 APR edition may be used until exhausted. All other editions are obsolete.

SECURITY CLASSIFICATION OF THIS PAGE: UNCLASSIFIED

UNDERCOOLING OF ALUMINUM ALLOYS, J. H. Perepezko, D. U. Furrer, Univ. of Wisconsin, Dept. Met. and Min. Eng., Madison, WI 53706 and B. A. Mueller, Battelle Laboratories., Columbus OH 43201-2693.

The development of refined microstructures for dispersion strengthening of Al alloys by rapid solidification is related to the undercooling at nucleation and during competitive crystal growth. With controlled droplet samples the important processing parameters that govern undercooling in the powders have been identified and include powder size and coating, melt cooling rate and superheat. The droplet method has yielded measured undercoolings of 175°C for Al and values near 300°C for some Al alloys. Droplet studies have been valuable in examining the solidification pathways including thermal history effects associated with rapid solidification and dispersoid formation in Al-Ni, Al-Fe, and Al-Be alloys. Based on the analysis of solidification pathways, microstructure maps may be developed to identify the processing that can yield fine-scale eutectics, metastable structures or suppression of coarse primary intermetallic phases which are useful for the development of dispersoid structures.

DISPERSION STRENGTHENED ALUMINUM ALLOYS

Y-W. Kim and W. M. Griffith, Editors

(TMS, Warrendale, PA)
pp. 77-102, 1988

Introduction

In the search for new materials, and microstructures, rapid solidification processing (RSP) has proved to be a very useful technique. During rapid solidification, the nucleation and growth of stable phases can be difficult. A wide range of reported microstructural variations encompass not only equilibrium phase mixtures with a refined microstructural scale, but also novel microstructures such as supersaturated solid solutions, metastable intermediate phases and amorphous solids.

Dispersion strengthened aluminum alloys can benefit from RSP techniques to produce the needed fine scale distribution of phases. At the same time the processing parameters which produce a desired microstructure need to be identified in order to predict and control microstructural development. Undercooling is one key processing parameter which is directly related to microstructural evolution. Through the control of melt undercooling, highly dispersed phase mixtures can be created by various phase separation reactions, fine scale eutectic growth, precipitation of phases from supersaturated solid solutions, or from the decomposition of metastable phases.[1]

With most RSP methods direct information on the specific solidification pathway and thermal history controlling microstructure development is not accessible by accurate measurement, but instead the processing history is inferred based upon deductions from post-solidification microstructures combined with heat flow analysis calculations. Although this approach is useful, the interpretation of the microstructural analysis and heat flow calculations is not always unambiguous. As a result, the optimization of processing and alloy design to yield a reliable control of dispersoid microstructure development has not been possible in all cases. At the same time, with droplet samples, controlled undercooling experiments with Al alloys have been established as an effective approach to optimizing processing parameters to yield a maximum undercooling behavior and a high level of microstructure refinement. Moreover, the microstructural morphologies that develop during solidification in undercooled droplets under slow cooling conditions have been shown to be comparable to the structures that evolve during rapid quenching of atomized powders. From these studies, information can be gained on alternative solidification pathways allowing for favorable microstructures to be developed and a basis may be generated for an effective RSP alloy design.

Aluminum Droplet Production And Processing Parameters

Large undercooling in aluminum samples can be achieved by dispersing a liquid sample into a large number of small droplets, with sizes 5 - 40 um, with only a small fraction of the droplets containing potent nucleants. If droplet independence can be maintained without introducing potent catalytic sites, then the effects of internal nucleants can be restricted to a minor fraction of the droplet population, and the majority of the droplets can display a large undercooling.

The Droplet Emulsion Technique (DET) is an effective means to produce aluminum powders on a laboratory scale. A schematic of the emulsion system is shown in figure 1. Powder is produced by melting an inorganic salt and alloy mixture in an alumina crucible. Inorganic salt systems were chosen for use as

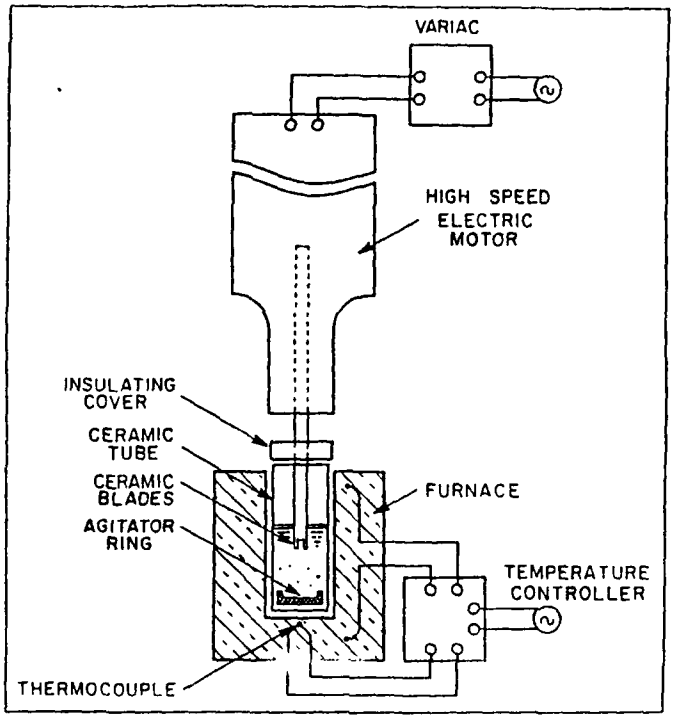

FIG. 1. Schematic diagram of the droplet emulsification apparatus.

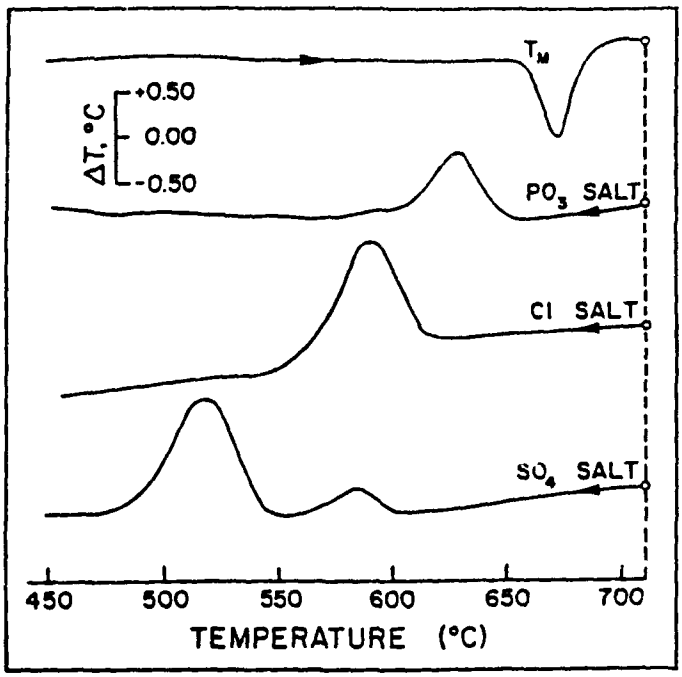

FIG. 2. DTA thermograms showing the variations in undercooling which results from producing aluminum powders in different inorganic salts.

the carrier media on the basis of a propensity for aluminum compound formation with the expectation that they may either modify or produce beneficial fluxing action on the oxide typically present on aluminum. The molten alloy and salt mixture at a superheat of 50-75°C is sheared into many fine droplets that are dispersed in the carrier media. Following the emulsification, the powders are retrieved by dissolution of the salt and subsequently the powders are collected, and sieved into size ranges.

The past experience with the droplet technique has identified a number of processing parameters that influence the optimization of liquid undercooling in powder samples. These processing variables include: droplet size refinement [2], melt superheat, melt cooling rate, alloy composition, as well as droplet surface coating [3,4].

Droplets size refinement tends to promote deep undercoolings. In general, the finer the size, the larger the undercooling. With melt superheat, the effect on the undercooling tends to be specific to the system. Each aluminum alloy system has a certain level of superheat which allows for the greatest undercooling. In general, increasing the cooling rate tends to increase the undercooling. Processes with very high cooling rates such as gas atomization make undercooling studies very difficult, because nucleation temperatures can not be measured. Powders processed in the DET are analyzed by Differential Scanning Calorimetry (DSC), Differential Thermal Analysis (DTA) or by a moderate quenching ($< 10^3$ °C/s) apparatus which give controlled cooling rates, and measured undercooling levels.

An important powder processing parameter is the powder coating. The coating is important in two respects. The first is due to the coating influence on the attainable undercooling level, and the second is related to the effects on the powder compaction characteristics [5]. Droplet coatings should be less catalytic than any internal nucleants in order to achieve high undercoolings and clearly the best coating is one that is inert catalytically. An effective method of controlling the aluminum powder coating chemistry is to change the chemical constituency of the environment in which the powders are produced. While atomization techniques typically use a gas environment, the droplet emulsion technique uses a liquid medium to produce powders. The different liquids used give rise to differences in the powder coating chemistry.

The undercooling response of aluminum powders produced in three different salt environments as measured in the DTA is shown in figure 2. Powders in each of the salts attain a distinct undercooling level with powders produced in the phosphate salt achieving the least undercooling, those produced in the chloride salt attaining an intermediate amount, and those powders produced in the sulfate salts achieving the largest undercooling.

As a means of investigating the different levels of undercooling induced by the different salts, as well as the ability of the chemical environment in which the powders are produced to alter the coating chemistry, powders were characterized by Auger Electron Spectroscopy (AES). The results of the surface chemistry analysis for powders made in each of the salts are shown in figure 3. The analysis indicates that while an Al_2O_3 oxide coating is detected on powders produced in each of the salts, differences in coating chemistry may be induced by varying the dispersal media chemistry. For example, the phosphate

salt gives rise to phosphorus being present in the surface, the sulfate salt leaves a sulfur residue while the chloride salt leaves traces of chlorine in the Al_2O_3 coating.

The increase in the undercooling level of the aluminum powders produced in the sulfate salt indicates that the sulfur present in the surface coating has modified it in some manner. A model has been proposed with which the surface modification can be explained [3]. From the work of Fletcher [6], nucleation on the surfaces of samples is initiated at conical pits as in a surface depicted in figure 4A. If the sulfur which is present after powder production in the sulfate salt resides on the ledges of the pits, the sulfur will in effect alter the pit size and distribution, as can be seen in figure 4B. The reduced pit size causes the radius of a nucleus which may form in it to be decreased. To compensate for the reduced nucleus radius, the undercooling prior to nucleation must be increased. Thus, the effect of the sulfate salt is to poison the catalytic sites present at the coating/liquid interface. This example illustrates one mechanism for surface coating modifications to yield a significant influence on the attainable undercooling, but other processes involving the distribution and potency of active surface sites [7] can also contribute to control of undercooling.

Even when these processing parameters are satisfied to produce large undercoolings, the vast amount of information suggests that solidification is initiated by heterogeneous nucleation at or near the surface of the droplets [8]. In these cases the maximum undercooling limit appears to represent the catalytic potency of the surface coating. Therefore, it appears that close attention to the nature of the coating is of prime importance in attaining reproducible, large undercooling levels.

Solidification of Al Alloy Powders

The undercooling experienced with pure Al is important to consider because a similar influence of powder processing parameters has been found to prevail in the treatment of Al-rich alloys. The solidification microstructure that develops in Al alloys has been documented to be related closely to the initial level of undercooling at the onset of solidification [9,10]. Of course, with alloy solidification the available pathways for freezing from an undercooled state involve a variety of options. In this case the microstructural and thermal history analysis capabilities that can be applied in the controlled solidification of droplets are of particular assistance in identifying the operative pathway under a given set of processing conditions. A number of the RSP pathway options can be analyzed by examining the solidification of droplet samples in several Al alloy systems which offer a useful potential for dispersoid formation.

Aluminum - Nickel Alloys

A number of useful starting structures for dispersion hardening have been produced in Al-Ni alloys including metastable intermetallic [11,12], supersaturated aluminum [13-15] and amorphous phases [16]. In powder form, aluminum-nickel alloys can be undercooled to relatively large levels which are comparable to levels attained in pure Al by controlling the powder

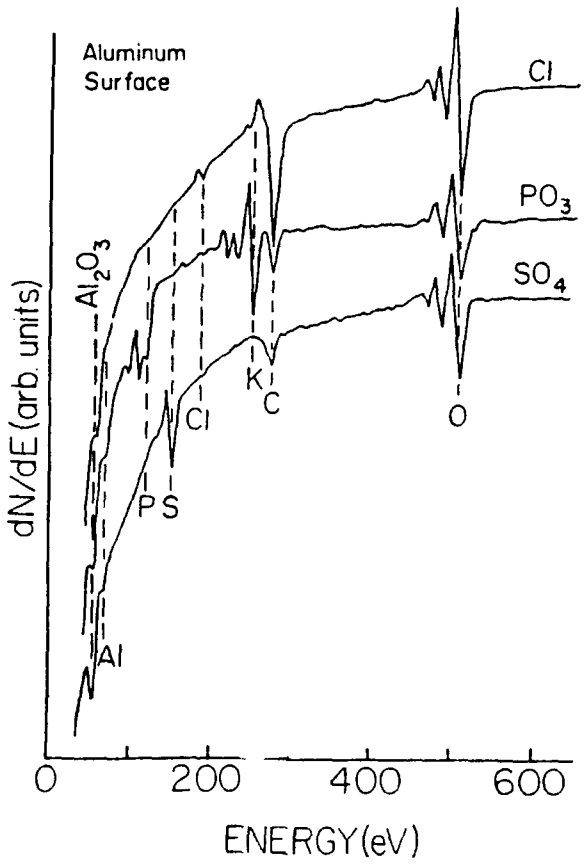

FIG. 3. AES spectra of the external surface of aluminum powder made in the various salts.

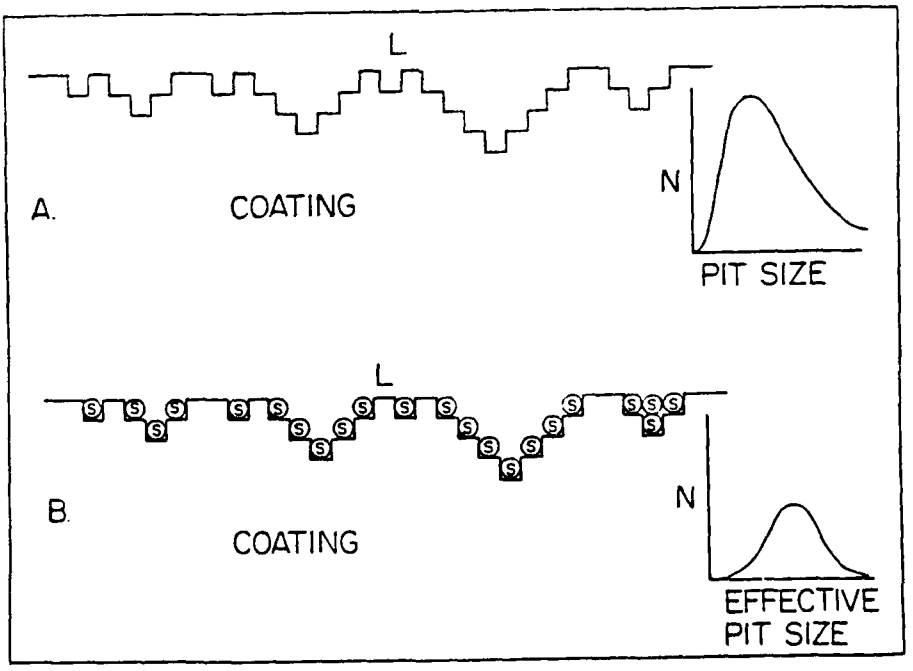

FIG. 4. Schematic of the liquid/coating interface of aluminum powders. (A) represents an interface without sulfur, while (B) indicates the sulfur addition.

processing parameters. In the present work, several unique features associated with refined microstructures appear in rapidly solidified Al-Ni powders with the Al-rich compositions near the Al/Al_3Ni eutectic.

Hypoeutectic alloy powders of Al-3 wt/o Ni were observed to undercool by 170°C and exhibit a single nucleation exotherm at a modest cooling rate of 500°C/sec. Figure 5A shows the typical microstructure developed in Al-3 wt/o Ni droplets, and illustrates a number of characteristic features of RSP powder microstructures. For example a gradation in structural refinement is apparent across the diameter of the internal section. The most highly refined structure appears to originate near the surface in the lower right section. Away from this starting point the cellular pattern exhibits an increasing cell size. This pattern of microstructural scale variation is expected from the recalescence thermal history associated with the initial adiabatic solidification of an undercooled powder [17]. Based upon X-ray measurements of the Al lattice parameter, the primary aluminum cellular region was supersaturated in excess of the equilibrium solubility. From a plot of the aluminum lattice parameter versus composition [18], the composition of the aluminum solid solution, was estimated as approximately 2 wt/o Ni. While the observed supersaturation is not the maximum level possible, it is consistent with solidification at the measured undercooling in terms of a metastable extension of the aluminum solidus.

The decomposition of the supersaturated powders was examined using DSC, which determined that the decomposition reaction is centered at about 400°C. A DSC thermogram is shown in figure 6 in which two peaks are evident. The lower temperature endotherm is due to the liberation of the water of hydration in the aluminum oxide powder coating [19]. The exothermic second peak corresponds to the decomposition of the supersaturated powder. Following the decomposition reaction at 400°C, X-ray diffraction lattice parameter measurements indicated that the Al solid solution had achieved the equilibrium solubility of near 0.05 wt/o Ni. The microstructure of the powder after decomposition treatment is presented in figure 5B. The size scale gradation that was present in the as-solidified microstructure has been obliterated following solid state heat treatment. The intercellular zone has been replaced by a collection of discrete dispersoids of the intermetallic Al_3Ni phase with sizes in the range of 0.04 to 0.7 um. Moreover, the low equilibrium solid solubility of nickel in aluminum is expected to facilitate retention of the dispersoid microstructure during consolidation [20].

The formation of a supersaturated Al solid solution is a useful precursor structure for the development of a high density of fine dispersoids by solid state heat treatment. As a result, it is of interest to compare the results on the maximum supersaturation level attained in a variety of rapid quenching methods. A plot of supersaturation level of nickel in aluminum as a function of cooling rate is shown in figure 7. This plot is composed of cooling rate, and supersaturation data from splat quenching, vapor deposition, and powder solidification work. A cooling rate of 10^7-10^8 °C/sec was reported as typical for one gun-splat quenching experiment [13]. For a two piston-splat quenching process an estimated cooling rate has been reported in the range of 10^5-10^8 °C/sec [12]. The cooling rate for a flash vapor deposition method [14] as well as that for

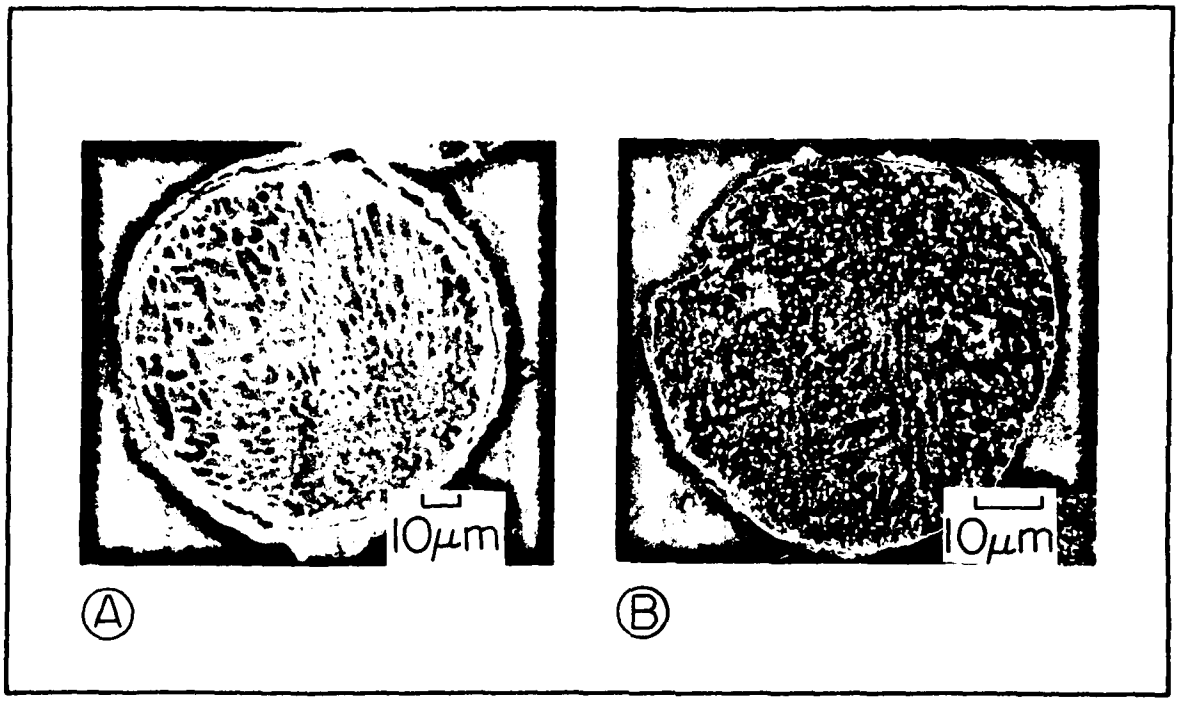

FIG. 5. (A) An Al-3 wt%Ni powder that was cooled at 500° C/sec. (B) An Al-3 wt%Ni powder that was cooled at 500°/sec, and decomposed in a DSC.

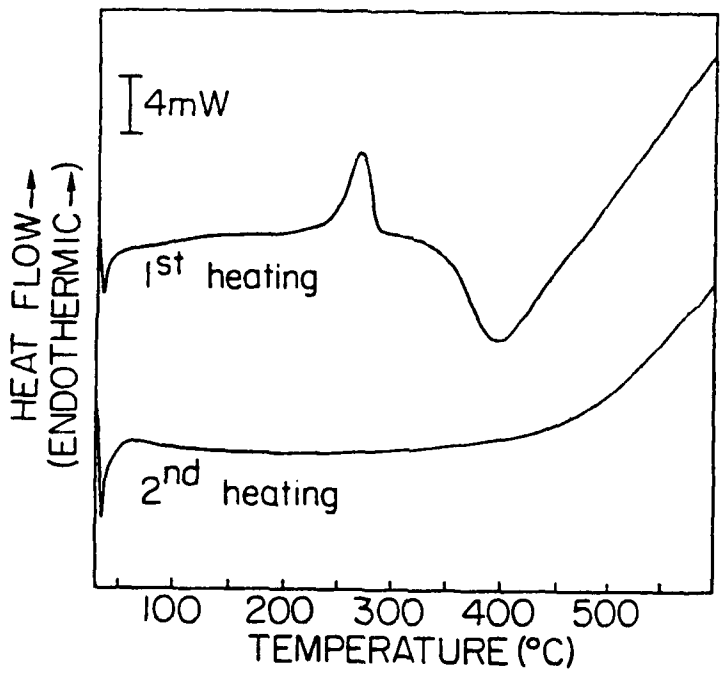

FIG. 6. DSC thermogram of the supersaturated Al-3 wt%Ni powder. The decomposition exotherm is centered about 400°C.

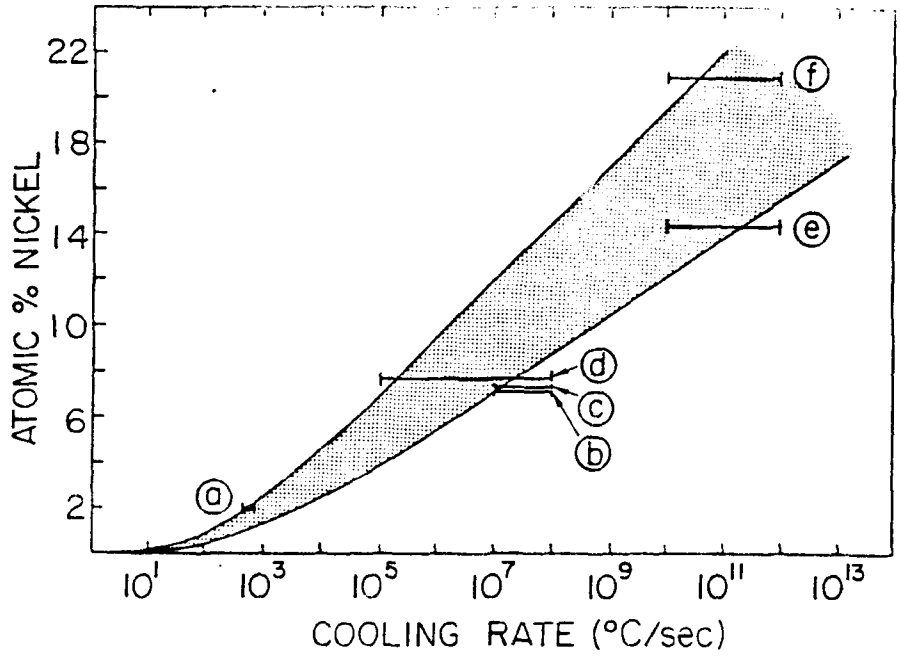

FIG. 7. A plot of the approximate relation between aluminum supersaturated, and processing cooling rate. (A) determined from the present work. (B) [11], (C) [13], and (D) [12] are from splat quenching work, while (E) [14], and (F) [15] are from vapor deposition studies.

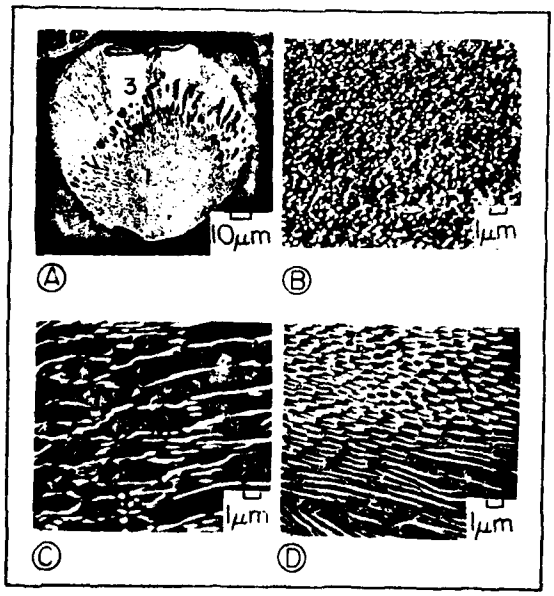

FIG. 8. Micrograph of an Al-6.1 wt%Ni powder depicting the three zone structure (A), where zone 1 (B) is a two phase morphology, zone 2 (C) is a cellular structure, and zone 3 (D) is the Al-Al_3Ni eutectic.

a vapor quenching treatment [15] can be estimated to be of order of about 10^{10}-10^{12} ^{o}C/sec. The cooling rate used in the present work was the measured value. The plot indicates that the degree of supersaturation of nickel in aluminum increases with increasing cooling rate in a continuous trend. At high cooling rates the scatter in the results due to the uncertainty in the value of the cooling rate is too great to conduct any detailed kinetics analysis. In fact, at the highest nickel levels and cooling rates, reported experience indicates that glass formation is also possible [16]. While metallic glass formation also signifies a supersaturation of Ni, the solidification mechanism is different than that yielding a metastable Al solid solution. Such a variability in structure formation suggests a sensitivity to sample conditions between different quenching methods. If this factor can be identified, then a master plot mapping supersaturation level at different quench rates can be established and analyzed based upon droplet results obtained at low cooling rates [21]. This type of master plot can be used to set processing conditions for the formation of supersaturated Al at a given level, and subsequent solid state precipitation of dispersoid phases can be performed to produce submicron dispersoids.

Alloys of eutectic composition have also been processed as droplet dispersions and were observed to exhibit a significantly different microstructural morphology than the hypoeutectic powders as illustrated in figure 8. Three microstructural zones can be observed. Nucleation occurred in zone 1, which exhibits a fine two phase morphology associated with an initial rapid solidification and recalescence. The fine-scale microstructure may have formed as a result of pinching off of deeply grooved Al cells [22], spheroidization of Al_3Ni rods that formed between the fine Al cells, or rapid nucleation and limited growth of Al_3Ni particles on the rapidly moving Al interface. A more detailed examination of the fine scale microstructure by TEM is in progress to establish the pathway for zone 1. With a change in the solidification conditions during recalescence and a reduced growth rate, a second microstructural zone develops which is composed of aluminum cells with intercellular Al_3Ni. During continued cooling the droplet completes solidification under external heat transfer in zone 3, which displays a eutectic morphology. It appears that the measured droplet undercooling levels reached a temperature where the growth of a two-phase Al/Al_3Ni structure was preferred, and upon recalescence the morphology changed to cells of aluminum with intercellular Al_3Ni, and upon final cooling the structure became a regular Al-Al_3Ni eutectic. The solidification path leading to zone 1 produces a very fine dispersion of Al_3Ni in the aluminum, which should act as a good dispersion strengthener.

Hypereutectic powders of compositions Al-9, and 12 wt/o Ni were also processed in controlled undercooling experiments and developed a multi-zone microstructural morphology. Powders of these compositions cooled at 500^{o} C/sec exhibited extra diffraction peaks in addition to those of Al and Al_3Ni upon x-ray analysis. The additional peaks have been indexed to correspond to the metastable intermediate phase Al_9Ni_2. The Al-Ni-Fe system [23] has an equilibrium ternary, monoclinic compound, $Al_9(Fe_xNi_{1-x})_2$ [24], which would correspond to Al_9Ni_2 upon extrapolation to the binary Al-Ni system. The Al_9Ni_2 compound has not been previously reported to exist in the Al-Ni binary, however a monoclinic phase of undetermined composition

was reported to develop after solid state decomposition of splat quenched Al-Ni [11].

The powders containing Al_9Ni_2 were analyzed with DSC. The powders exhibited a single, well-defined exothermic peak centered at about 375°C. Upon subsequent X-ray analysis the Al_9Ni_2 peaks were absent. The metastable phase(s) obtained in other studies were reported to decompose between 150-300°C with isothermal treatments [11,12,25].

The microstructure developed in Al-12 wt/o Ni powders that were undercooled 200°C below the liquidus is shown in figure 9. Again the powders appear to exhibit a three zone microstructure, where zone 1 represents a coupled morphology, zone 2 is a primary intermetallic phase, and zone 3 is a coupled eutectic structure. Zone 1 is presumed to correspond to the coupled growth of the Al-Al_9Ni_2 metastable eutectic, which becomes less preferred upon recalescence outside of the coupled zone and forms primary dendrites of Al_9Ni_2. The powder finishes solidification in zone 3 with the control of the growth by external heat flow which allows the coupled growth of the Al-Al_3Ni stable eutectic. The determination of the coupled growth zone, the temperature/composition region in a phase diagram where the growth of a coupled eutectic structure is faster than either primary phase, is important when fine scale dispersions microstructures are desired. When the coupled zone is mapped out, a cooperative growth morphology can be obtained in alloys other than the eutectic composition when the processing conditions allow the alloy to solidify within temperature/composition region of the coupled zone. The aluminum side of the Al-Ni phase diagram with the possible coupled zones of the stable Al-Al_3Ni eutectic, and the metastable Al-Al_9Ni_2 eutectic is shown in figure 10. The metastable liquidus was determined from extentions of the ternary liquidus isotherms, along with the metastable peritectic and eutectic reactions [23,26,27]. The metastable phase was observed in compositions around the metastable eutectic because the undercooling needed to reach the metastable liquidus is the least in this range of composition. Since the eutectics are of a facetted/non-facetted type it is expected that the coupled growth zones will be skewed in the direction of the intermetallics due to growth kinetic reasons [28].

Powders of 15 and 19 wt/o Ni were observed to contain a two zone microstructure. Zone 1 was composed of a coupled morphology which develops into the zone 2 structure composed of dendrites of Al_3Ni and interdendritic eutectic. The hypereutectic powders nucleated and grew with a coupled Al-Al_3Ni morphology until the temperature was increased sufficiently by recalescence to make the coupled morphology less preferred, leading it to the formation of dendrites of Al_3Ni, and interdendritic eutectic. Powders greater than 19 wt/o Ni did not exhibit a coupled morphology with the undercooling levels observed. These alloys nucleated and grew as dendrites of Al_3Ni with interdendritic eutectic.

Aluminum - Iron Alloys

Rapidly solidified Al-Fe alloys are an important class of aluminum alloys since RSP can effectively bypass formation of coarse, brittle Al_3Fe which is produced during conventional processing of these alloys [29,30]. The avoidance of the Al_3Fe primary in rapidly solidified Al-Fe alloys allows for the for-

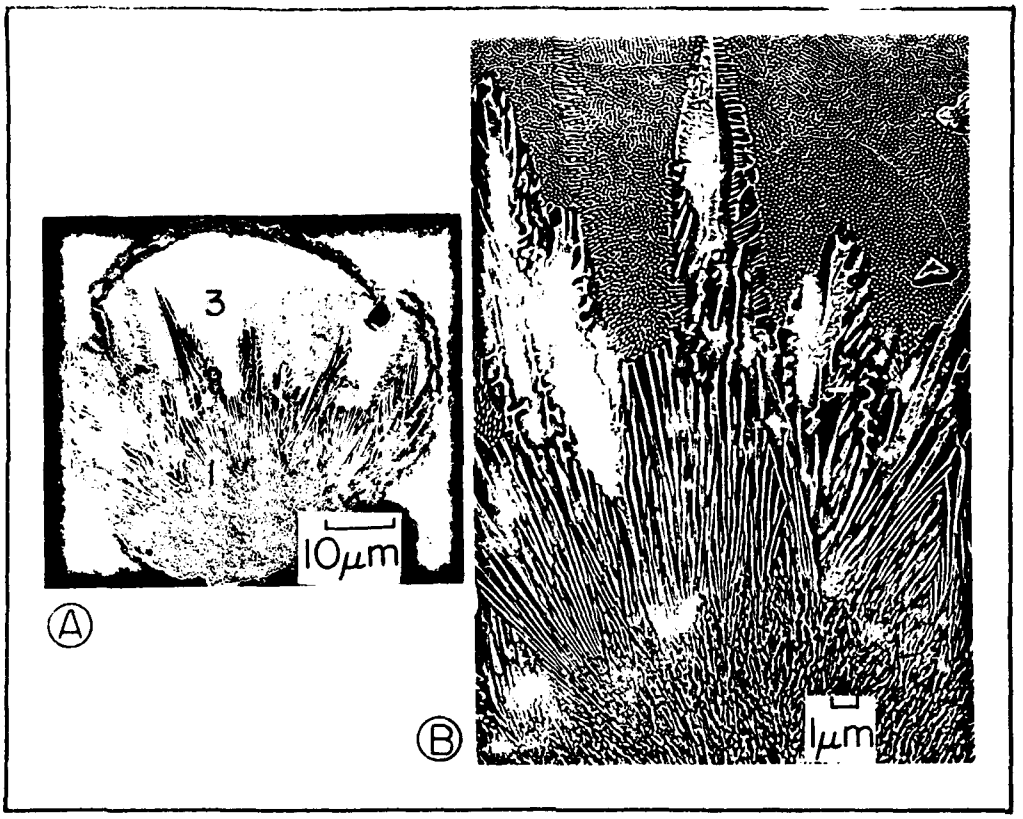

FIG. 9. Micrograph of an Al-12 wt%Ni powder (A and B), in which initial solidification was the metastable Al-Al_9Ni_2 eutectic in zone 1. Zone 2 is a region in which dendrites of Al_9Ni_2 formed. Zone 3 is a region of stable eutectic.

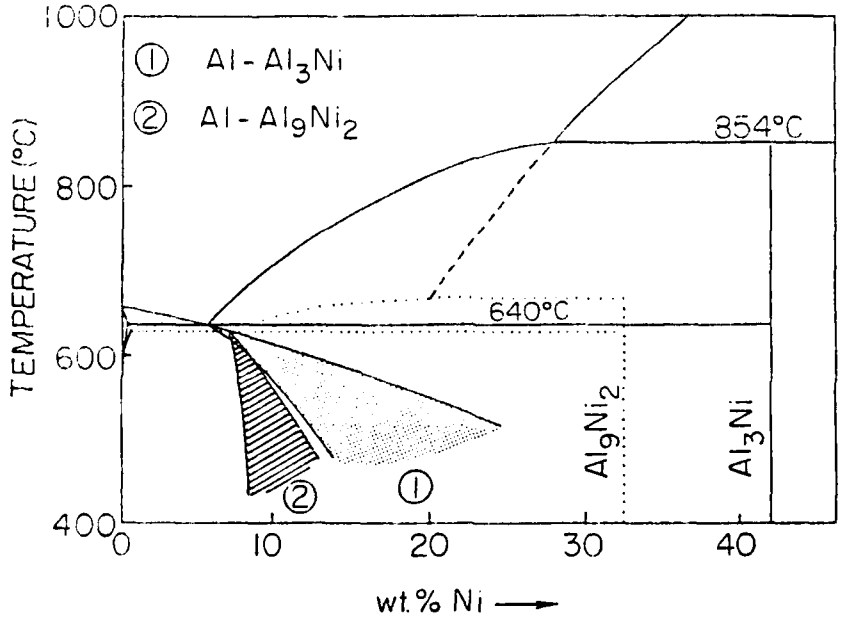

FIG. 10. The aluminum side of the Al-Ni phase diagram which includes the metastable phase Al_9Ni_2 and the possible coupled growth zones of the stable and metastable eutectic.

mation of the metastable Al_6Fe phase, and the Al-Al_3Fe eutectic. This eutectic is formed in both slowly cooled and atomized powders, and has been found to be kinetically stable up to the measured metastable eutectic temperature at 649°C during continuous heating in DTA examinations. Figure 11 shows the Al rich side of the Al-Fe phase diagram with the possible coupled zones of the stable Al-Al_3Fe eutectic and the metastable Al-Al_6Fe eutectic [29].

To exemplify the importance of undercooling on the microstructural formation, the microstructure developed in slowly cooled Al-Fe powders has been compared to atomized powders [31]. Figure 12 shows that in slowly cooled Al-Fe droplets the primary Al_3Fe phase can be avoided, and a fine scale microstructure develops. The fine structure is composed of aluminum cells followed by the formation the metastable Al-Al_6Fe eutectic. Similar fine structures are seen in atomized powders as in figure 13. The rapidly quenched atomized powders form a fine scale mixture of Al and Al_6Fe also with the avoidance of Al_3Fe.

Powder coating modifications can be produced by altering the chemical environment in which the powders are emulsified. Coating modifications may also be affected by the addition of solute prior to emulsification. One such solute addition is cerium. The undercooling results of Al-9.0Fe powders, and Al-8.4Fe-7.0Ce powders of similar sizes analyzed under similar conditions are compared in figure 14 for cooling from the liquid region, and also from the liquid plus Al_3Fe region. The undercooling results of the Al-9.0Fe seem to indicate that the undercooling is limited by primary phase formation. Figure 15 shows the microstructure in Al-9.0Fe powder what was held in the liquid plus Al_3Fe region and cooled in order to evaluate the undercooling of the liquid in the presence of a primary phase. This DTA treatment is termed a heterogeneous cycle (HET cycle). The HET cycle of the sample with Ce addition gave similar undercoolings, but the DTA trace for the complete thermal cycle indicates a much greater undercooling. It seems that the addition of cerium allows for the avoidance of the primary Al_3Fe intermetallic upon continuous slow cooling, which permits the powders to attain an increased undercooling. A nucleation temperature of 560°C corresponding to an undercooling of 320°C below the liquidus is equivalent to an undercooling of $0.28T_m$ for this alloy. The microstructure of the highly undercooled powders exhibited no coarse intermetallic constituent, but rather a fine structure composed of cells of aluminum and intercellular intermetallic.

Aluminum - Beryllium Alloys

Aluminum-Beryllium is an alloy system which is quite attractive from a rapid solidification processing approach. The low density and relatively high elastic modulus of beryllium allow for the potential to produce stiff alloys with a very high strength to weight ratio [32]. With conventional processing conditions this system is of little interest because the maximum solid solubility limit of beryllium in aluminum and the eutectic composition lie too low to produce either effective solid solution or dispersion hardening. However, by employing rapid solidification techniques to these alloys it is possible to increase the level of beryllium in solid solution or to increase the beryllium content dispersed uniformly

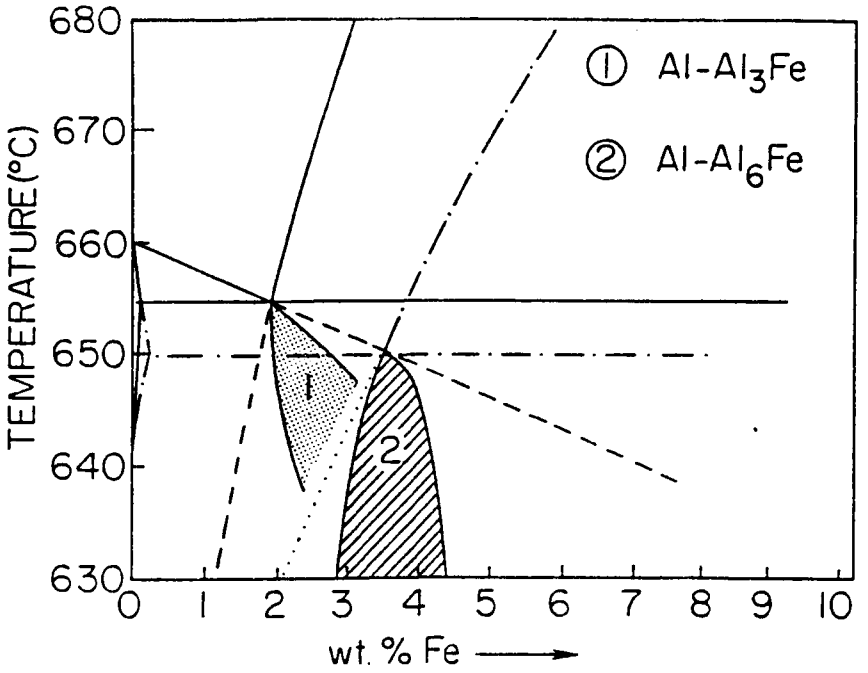

FIG. 11. The aluminum side of the Al-Fe phase diagram with the possible coupled growth zones of stable Al-Al_3Fe eutectic, and the metastable Al_6Fe eutectic.

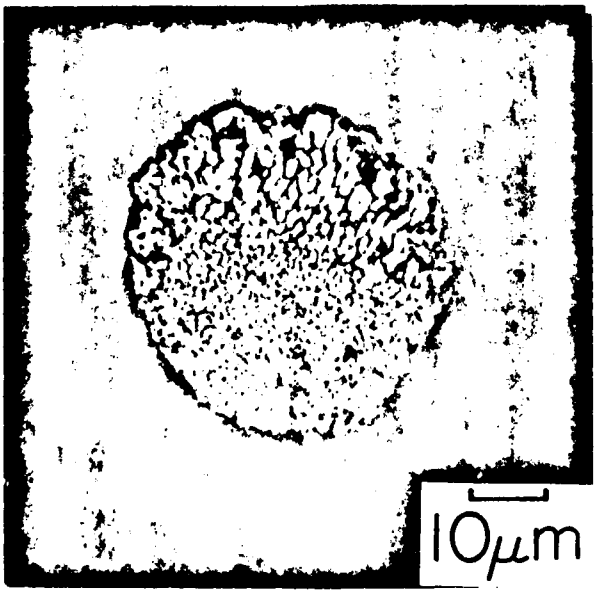

FIG. 12. Refined microstructure developed in undercooled Al-5 wt%Fe powders cooled at 0.5°/sec.

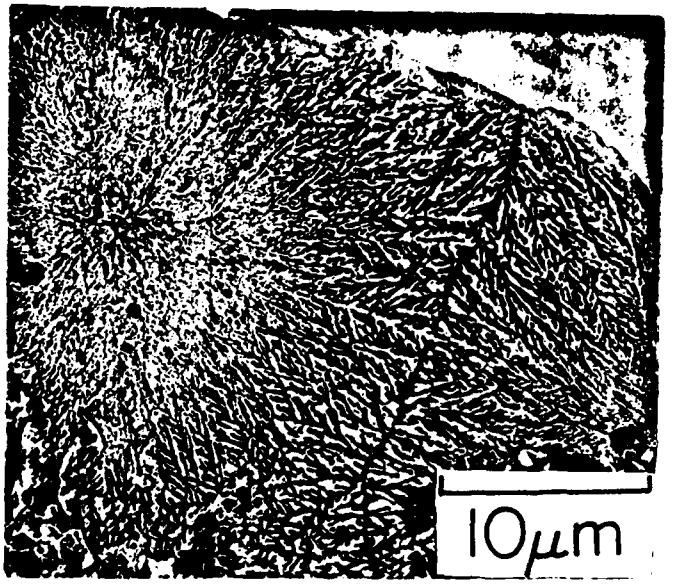

FIG. 13. An atomized Al-9 wt%Fe powder showing a refined microstructure with a radiating recalescence structure.

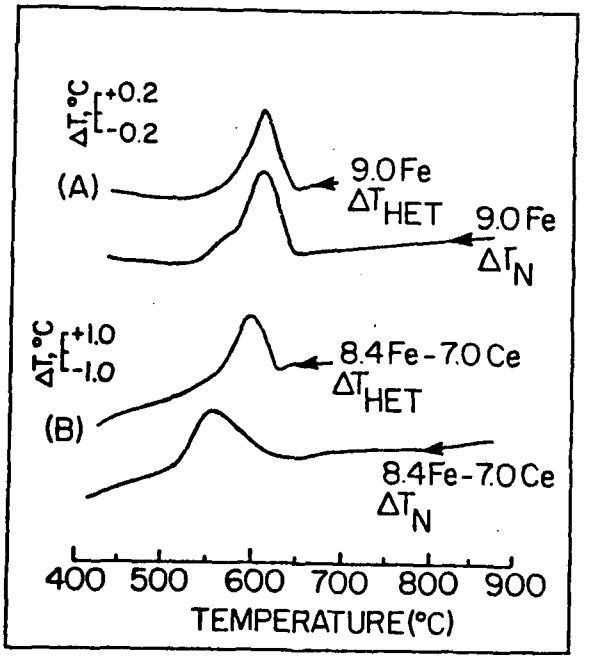

FIG. 14. DTA thermograms demonstrating that primary phase formation limits the undercooling of Al-9 wt%Fe powders (A), while the addition of cerium allows for the avoidance of the primary phase and an increased undercooling in powders undergoing the maximum undercooling treatment (B).

and finely throughout an aluminum matrix.

Powders of several compositions up to 15 at%Be were produced using the droplet emulsion technique. It was observed that the undercooling of the aluminum was altered with the addition of beryllium by the change of the measured 175°C undercooling of pure Al to 97°C below the liquidus for the alloy. The change in undercooling appears to be related to a change in droplet surface chemistry as shown in figure 16, which compares the auger electron spectra of the surface of pure aluminum and Al-10 at%Be powders processed in the same salt under similar conditions. It can be seen that the powders produced from the beryllium containing alloy do not possess a complete aluminum oxide coating, but rather exhibit a beryllium oxide coating. It appears the beryllium oxide has nearly completely displaced the aluminum oxide surface coating.

The measured undercooling for the Al-10 at%Be powders varied from 15°C for powders cooled at a rate of 0.5°C/sec, to 97°C for powders cooled at 500°C/sec. The increase in undercooling with the increase of cooling rate also brought about microstructural differences. The alloys cooled at 0.5°C/sec contained primary beryllium followed by cells of aluminum and eutectic. Powders that were cooled from the liquid plus beryllium region (HET cycle) also exhibited primary beryllium, however the primary phase facets were more completely developed than in the samples that were continuously cooled from the liquid. An example of well developed facets on a primary Be particle is given in figure 17 for an Al-9 at%Be powder that was treated with a HET cycle which allows additional time in the (L + Be) region, for development of the facets compared to continuous cooling. When the aluminum-beryllium powders were cooled at 25°C/sec the development of facets on the primary beryllium phase was limited and a non-facetted dendritic morphology was evident. The higher growth rate also causes the cellular aluminum and intercellular eutectic to become much finer than those of the samples cooled at 0.5°C/sec.

In Al-9 at%Be powders that were cooled at 500°C/sec, a large number of primary beryllium particles were observed, and many of these possess a classic dendritic solidification morphology. Multiple primary nuclei are uncharacteristic of powder samples because typically a single nucleation event occurs in undercooled samples [8]. The formation of multiple primary particles may be due to the increased undercooling and is being examined further [33]. In other hypereutectic alloys, with a decreasing Be content, a significant change in initial phase selection and subsequent microstructure development was observed in undercooled powders. For example, an analysis of Al-4 at%Be powders cooled at 500°C/sec revealed that nucleation commenced with an aluminum cellular structure followed by a region of eutectic. A region in an Al- 4at% Be alloy powder, where a fine eutectic structure was formed, is presented in figure 18. In this case a uniform array of Be rods with sizes in the range of 30-50 nm, and an area density of about 1×10^{13} m^{-2} is evident. Thus, a high density of fine beryllium rods at compositions in excess of the equilibrium eutectic are attainable which gives these alloys the potential for effective dispersion hardening.

The aluminum-beryllium system also possesses the potential for a number of interesting different solidification pathways, due to the numerous metastable equilibria which exist in this system. The metastable equilibria can develop under con-

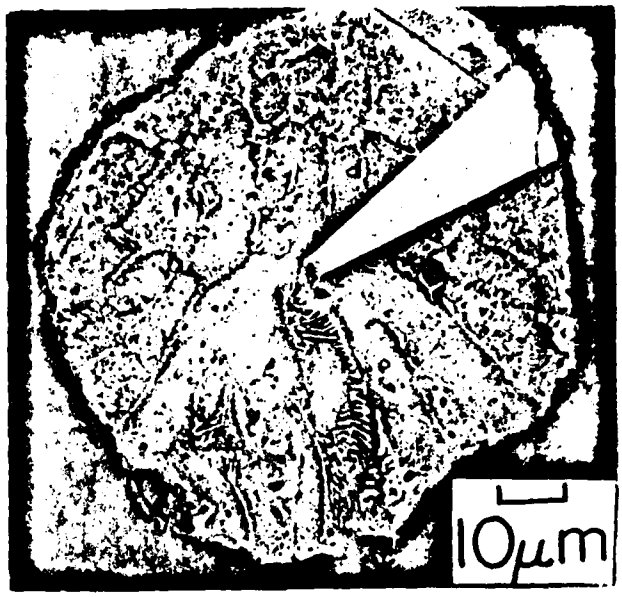

FIG. 15. An Al-9 wt%Fe powder slow cooled showing a primary Al_3Fe plate, cells of aluminum, and Al-Al_6Fe eutectic.

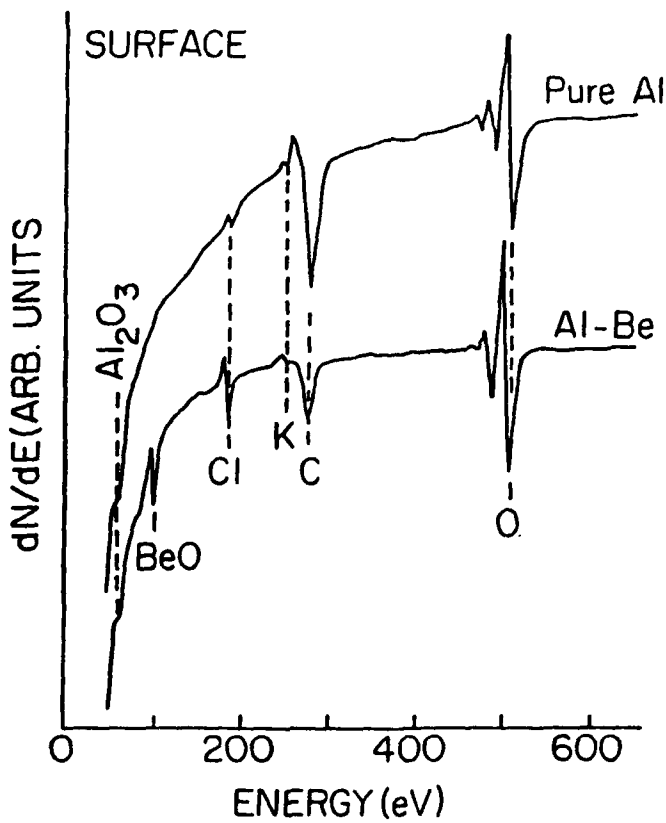

FIG. 16. AES spectra showing the change in the surface coating resulting from the addition of Be to an Al ingot.

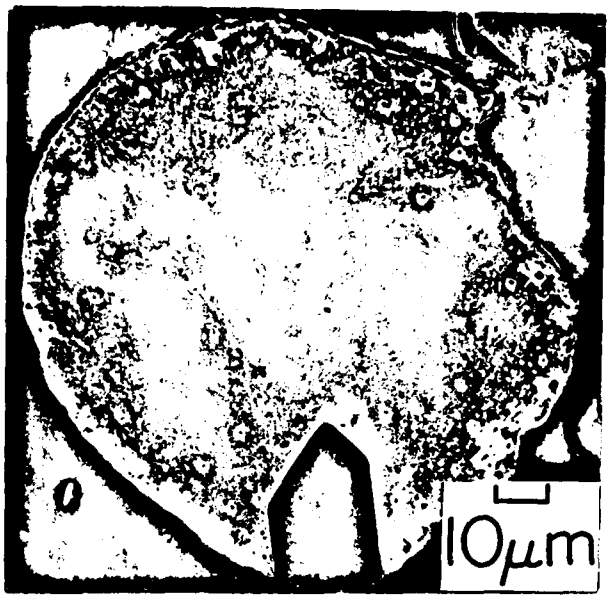

FIG. 17. Micrograph of an Al-9 at%Be powder after a heterogeneous DTA treatment showing a facetted Be primary.

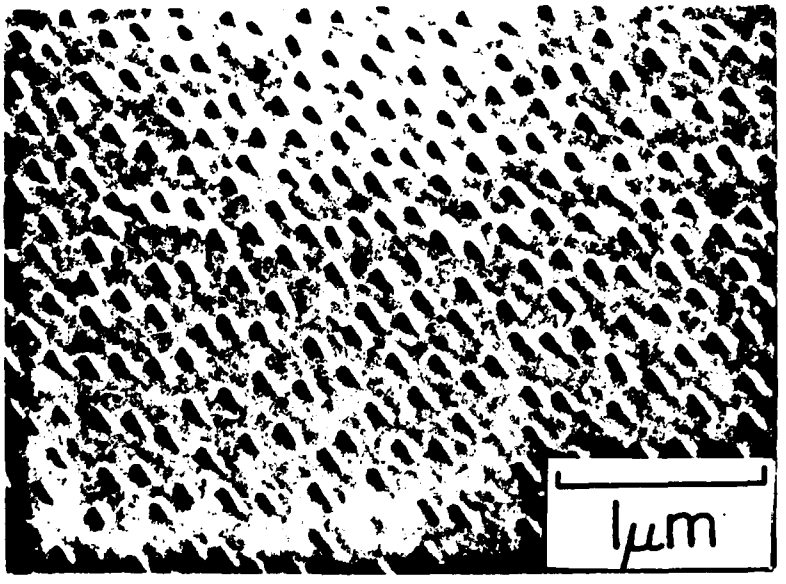

FIG. 18. Micrograph of an Al-4 at%Be powder showing fine rods of beryllium dispersed in aluminum.

straints related to the absence of a stable phase due to sluggish nucleation, and growth kinetics. The solidification pathways depend on the undercooling, and competitive nucleation and growth kinetics, which are also dependent upon processing conditions. The Al-Be phase diagram is shown in figure 19A with the addition of metastable equilibria lines calculated from thermodynamic considerations [34]. The two reactions depicted on the aluminum side are the stable Al(fcc)-Be(hcp) eutectic, and the metastable Al(fcc)-Be(bcc) eutectic as shown in detail in figure 19B. There are several other calculated metastable reactions in this system, including a monotectic involving a miscibility gap.

Under equilibrium conditions nucleation of primary hcp Be will occur at the liquidus temperature for hypereutectic alloy compositions. With continued cooling the liquid composition will follow the stable liquidus curve and the final solidification will occur at the eutectic temperature. If nucleation of the hcp Be is difficult, then the liquid can be undercooled below the stable liquidus. When the liquid is undercooled below the metastable bcc liquidus, it is possible to form primary bcc beryllium, and in fact bcc beryllium has been reported to form in surface melted samples [35].

Kinetic factors also influence microstructural development as demonstrated in Al-4 at%Be powders cooled at 500°C/sec. Even though the powder composition is hypereutectic, primary Be was not observed to form, but instead the first phase to form is aluminum with a cellular morphology. Thus, initial nucleation occurred below the extended Al liquidus. During the recalescence period following nucleation, the interface growth conditions changed, allowing for the growth kinetics of the eutectic structure to surpass those of the cellular aluminum upon entering the coupled eutectic growth zone, therefore the eutectic structure was formed.

In contrast, in melt-spun 4.4 at% Be ribbon [35] solidification was observed to commence with a eutectic-type structure, and recalescence caused the adoption of a cellular Al structure in the latter regions to solidify. Since the initial solidification of the hypereutectic ribbons was two phase, and the later stages cells of aluminum, it was presumed that they could not have formed by a eutectic reaction, but rather the results were interpreted in terms of a metastable monotectic reaction. Thus even though the composition of the powder and the ribbon were similar and the structures possessed many of the same features (cells of aluminum and two phase Al+Be regions), the pathways in which these structures developed are clearly different. In fact, the analysis capability that may be applied with droplet samples provides valuable guidance in establishing the availability of different pathways with different processing approaches. Clearly, all rapid solidification processing methods are not equivalent. This exemplifies a principal advantage of rapid solidification, to provide access to an increased number of potential solidification pathways.

Summary

From the controlled undercooling experiments on aluminum based alloys several important factors emerge in controlling the undercooling and subsequent microstructure development for dispersoid formation. One of these processing parameters is cooling rate. In general, undercooling is increased with

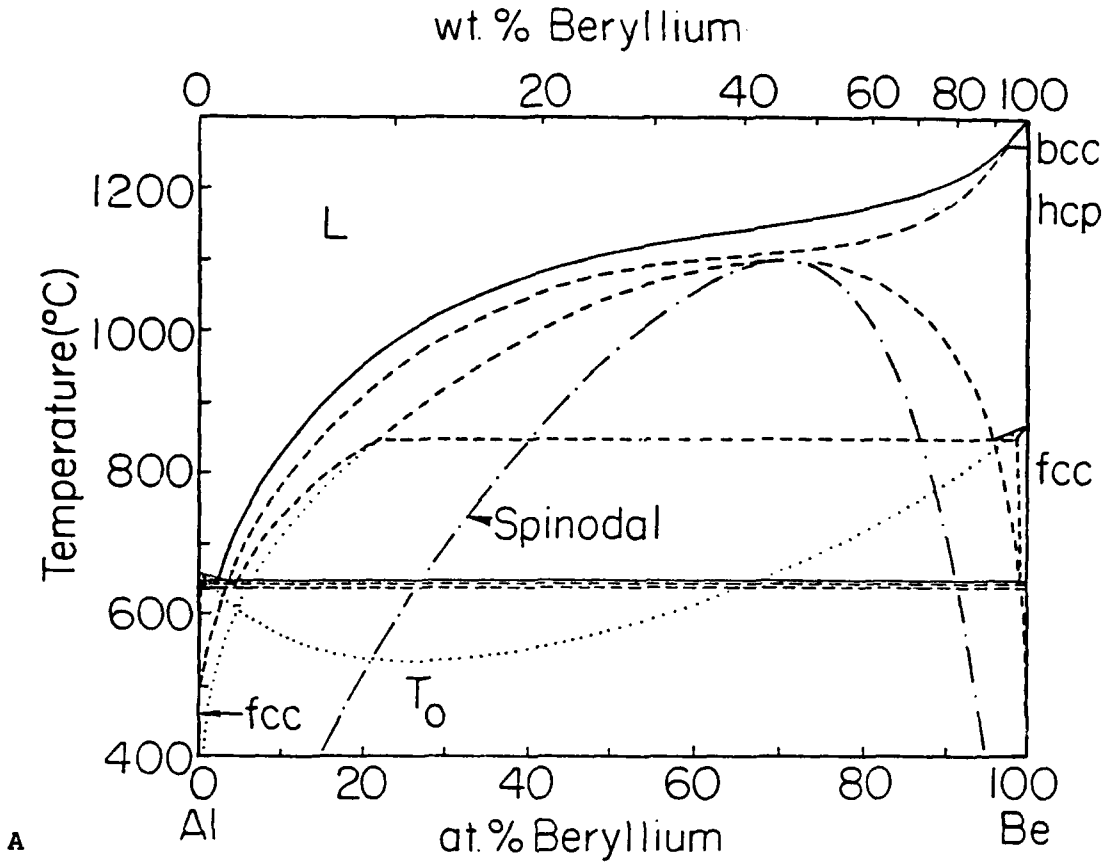

A

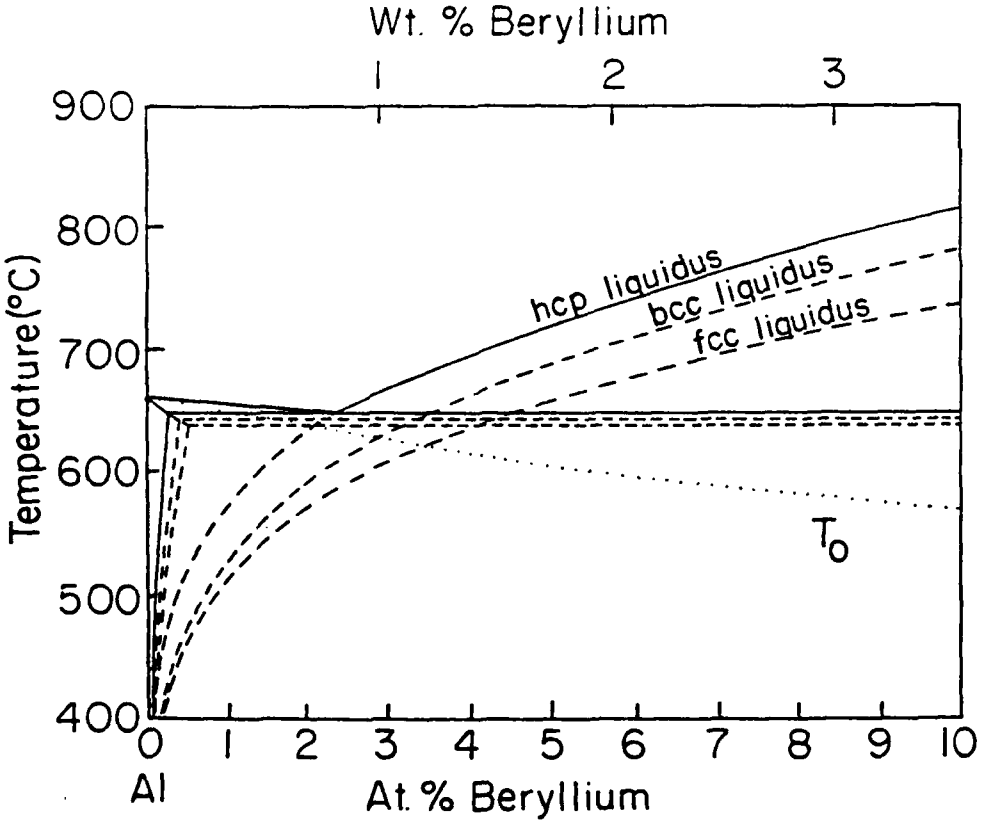

B

FIG. 19. The Al-Be phase diagram including calculated metastable equilibria (A), along with an enlargement of the aluminum-rich side of the diagram (B).

increased cooling rate, which allows for the possibility of additional pathways to be effective. Also, fine scale solidification structures are preserved to a greater extent if the heat extraction is rapid. Alloys that are cooled at slow rates, and are undercooled to high levels will solidify rapidly, however post solidification heat treatment may affect the microstructure and cause decomposition of metastable phases, and coarsening.

In a similar manner, coating effects become very important when large undercoolings are being examined. The media in which the powders is produced greatly affects the surface coating, and subsequently the undercooling. Solute additions also influence the coating and undercooling as demonstrated by the addition of cerium to Al-Fe alloys, and the addition of beryllium to aluminum. Subsequent processing during consolidation is also sensitive to powder coating variations; especially for Al alloys.

The consideration of metastable phase diagrams has provided valuable guidance in defining the range of operating kinetics and the reaction pathways for many solidification processes. The Al-Ni, Al-Fe, and Al-Be systems all exhibit metastable phase formation which is associated with dispersoid development, so that the corresponding metastable phase diagrams become important when working with RSP and high undercooling levels. Indeed an examination of the metastable diagrams in figures 10, 11, and 19 indicates that the potential influence of the metastable structures becomes most significant in the Al-rich composition range due to the modest undercooling required to allow for development of different metastable eutectics. The clear trend for development of metastable phase structures and other refined dispersoid phases at large undercoolings is apparent in the microstructural summary presented in Table 1 for a number of Al alloys that have been examined in droplet studies. The characteristic of powder solidification from an undercooled liquid to yield zones of different microstructural morphology and structure is also apparent from the listing in Table 1. The microstructural zones are developed in response to the thermal history associated with recalescence, competitive kinetics and external cooling. The microstructural variety is clearly one of the benifits of rapid solidification and provides an incentive for a more detailed analysis of the solidification behavior.

While significant progress has been made in acheiving dispession hardened Al alloys with useful properties by RSP, experience also reveals a number of issues that need to be addressed in developing a more reliable process control. For example, it is becoming clear that not all RSP methods are equivalent in terms of microstructural development. When the microstructural differences are examined in terms of cooling rate which is often similar for different methods, it is not clear how to resolve the apparent disparity. However, when microstructure development is considered in terms of undercooling, heat transfer, competitive growth, and metastable phase diagrams, it is evident that different pathways to either similar or to different structures can be selected at different undercooling levels and kinetic constraints even at for similar cooling rates. This is an important step towards the realization of processing maps for selected microstructures. Similar methods for solid state treatments may be developed to include the effects of metastable phase decomposition and precipitate

coarsening. Within this framework, a microstructure design strategy can guide processing in order to alter the melt surface or heat transfer and to select alloying additions that modify the nucleation kinetics, relative interface velocity and solid state stability of competing alternative structures that can be useful for dispersoid development.

TABLE 1

Summary of Droplet Microstructures

Alloy	Undercooling (^{o}C)	Microstructural Features
Al-Ni		
3wt%Ni	170	Formed supersaturated cells of Al. Precipitation of Al_3Ni observed upon DSC analysis.
6.1wt%Ni	160	Exhibited a multi-zone microstructures which contained 50 -100 nm diameter Al_3Ni particles.
9-12wt%Ni	200	Contained the metastable Al_9Ni_2 phase.
15-19wt%Ni	210	Coupled Al/Al_3Ni morphologies were exhibited.
Al-Fe (hypereutectic)	260	Formation of submicron particles of the metastable Al_6Fe phase.
Al-Fe-Ce (hypereutectic)	320	Suppression of primary Al_3Fe, with a cellular and eutectic structure.
Al-Be (4-15 at%Be)	97	Formation of a finely spaced eutectic (125-150nm) at compositions greater than the eutectic composition.
Al-Y [36] (eutectic)	60	Formation of a submicron dispersoids of Al_3Y in an Al matrix by rapid eutectic growth.
Al-Si [31] (up to 20 wt%Si)	160	Formation of 0.1 to 2.0 micron dispersoids of non-facetted Si in aluminum.

Acknowledgment

The authors thank Dr. W.J. Boettinger of NBS and Prof. S. Bailey of Univ. of Wisc-Madison, Dept. of Geology for their help and insightful discussion. The support of the U.S. Army Research Office (DAAL03-86-K-0114) is gratefully acknowledged.

References

1 P. Duwez, ASM Trans, vol 60, 1967, 607-633.

2 J.H. Perepezko and S.E. LeBeau, Proc. of Second Int. Symposium on Al Trans. Tech and Its Applications, eds. C.A. Pampillo, H.Billoni, and L. F. Mondolfo (ASM, Metals Park, OH) 309 (1982). Argentina, 1981.

3 B.A. Mueller, PhD thesis, University of Wisconsin-Madison

4 B.A. Mueller and J.H. Perepezko, Met. Trans A, 18A, June 1987, p. 1143.

5 W.M. Griffith, W. Kim, and F.H. Froes in Rapidly Solidified Powder Aluminum Alloys, ASTM, STP 890, M.E. Fine and E.A. Starke, Jr., Eds, Philidelphia, 1986, pp 283-303.

6 N.H. Fletcher, J. Atmospheric Sci., 26, 1969, 1266.

7 D. Turnbull, Acta Met. 1, 8, 1953.

8 J.H. Perepezko, B.A. Mueller, and K. Ohsaka, in Undercooled Alloy Phases, E.W. Collings and C. Koch, eds., TMS-AIME, Warrendale, PA, 1986.

9 W.J. Boettinger, and J.H. Perepezko, in Rapidly Solidified Crystalline Alloys, P.21, S.K. Das, B.H. Kear and C.M. Adams, eds., TMS-AIME, Warrendale, PA, 1985.

10 J.H. Perepezko and W.J. Boettinger, in Surface Alloying by Ion, Electron, and Laser Beams, L.E. Rehn, S.T. Picraux and H. Wiedersich, eds., ASM, Metals Park, OH, 1986.

11 K. Chattopadhyay, P. Ramachandrarao, S. Lele, amd T.R. Antharaman, Proc. of Second Int. Conf. on Rapidly Quenched Metals, 1976, pp 157-61.

12 A. Tonejc, D. Rocak, and A. Bonefacic, Acta Met., 19, 1971, pp 311-316.

13 R. Hailes, J.H. Vincent and H. Jones, Proc. of Third Int. Conf. on Rapidly Quenched Metals, ed., B Cantor, 1, 1978, pp 163-6.

14 D. Duzevic, A. Bonefacic, D. Kunstelj, Scripta Met., 7, 1973, pp 883-6.

15 B. Cantor and R.W. Cahn, J. of Mat. Sci., 11, 1976, pp 1066-1076.

16 S.T. Picraux amd D.M. Follstaedt, Mat. Res. Soc. Proc., vol. 13, 1983.

17 W.J. Boettinger, and J.H. Perepezko, in Rapidly Solidified Crystalline Alloys, eds. S.K. Das, B.H. Kear, and C.M. Adam (TMS-AIME, Warrendale PA) 21 (1985)

18 F.D. Lemkey, R.W. Hertzberg and J.A. Ford, Trans. AIME, vol. 233, 1965, pp 334-341.

19 T. Sato, J. of Thermal Analysis, vol. 32, 1987, pp 61-70.

20 Y-W. Kim and F.H. Froes in Undercooled Alloy Phases, p. 395, E.W. Collings, and C.C. Koch eds., TMS-AIME, Warrendale, Pa, 1896.

21 B.A. Mueller, J.J. Richmond, and J.H. Perepezko, "Rapidly Quenched Metals V", eds: S. Steels, and H. Warlimont, Elsevier Sci. Pub., Amsterdam (1985), 47.

22 W.J. Boettinger, L.A. Bendersky, R.J. Schaefer and F.S. Biancaniello, to be published in Met. Trans. A.

23 V.G. Rivlin and G.V. Raynor, Int. Met. Rev, vol. 3, 1980, pp 79-93.

24 Y.W. Kim and A.G. Jackson, Scripta Met., vol. 20, 1986, pp 777-782.

25 D. Kunstelj and A. Bonefacic, Microstructural Sci., vol. 3, 1975, pp 207-215.

26 J.H. Perepezko and W.J. Boettinger in Alloy Phase Diagrams, vol. 19, eds. L.H. Bennett, T.B. Massalski, and B.C. Giessen, 1983, 223-240.

27 H.W.L. Phillips, Annotated Equilibrium Diagrams of Some Aluminum Alloy Systems, (The Institute of Metal, London, 1959).

28 W. Kurz and D.J. Fisher, Inter. Met. Rev., 1979, nos. 5-6.

29 C.M. Adams and L.M. Hogan, J. of Aust. Inst. of Metals, 17, 1972.

30 I.R. Hughes, and H. Jones, J. Mat. Sci., 11, 1976.

31 J.H. Perepezko, S.E. LeBeau, B.A. Mueller, and G.J. Hildeman, in Rapidly Solidified Powder Aluminum Alloys, p 118, M.E. Fine and E.A. Starke, Jr., eds., ASTM-STP 890, Philidelphia, PA, 1985.

32 W.E Quist and R.E. Lewis, in Rapidly Solidified Powder Aluminum Alloys, p 7, M.E. Fine and E.A. Starke Jr., eds., ASTM-STP 890, Philidelphia, PA, 1985.

33 B.A. Mueller, L.E. Tanner, and J.H. Perepezko to be pub-

lished.

34 J.L. Murray, private communication.

35 D. Van Aken and H. Fraser, in Undercooled Alloy Phases, E.W. Collings and C.C. Koch, eds., TMS-AIME, Warrendale, PA, 1986, p 413.

33 S.P. Ryan and J.H. Perepezko, unpublished research.